Supporting Information

Defects Passivation and Crystal Growth Promotion by Solution-Processed K Doping Strategy toward 16.02% Efficiency Cu(In,Ga)(S,Se)$_2$ Solar Cells

Yun-Hai Zhao[a, b, c, 1], Qian-Qian Gao[a, 1], Sheng-Jie Yuan[a, *], Qian-Qian Chang[a], Ting Liang[a], Zheng-Hua Su[b], Hong-Li Ma[c], Shuo Chen[b], Guang-Xing Liang[b], Ping Fan[b], Xiang-Hua Zhang[c], and Si-Xin Wu[a, *]

[a]Key Laboratory for Special Functional Materials of MOE, National & Local Joint Engineering Research Centre for High-efficiency Display and Lighting Technology, School of Materials, Collaborative Innovation Centre of Nano Functional Materials and Applications, Henan University, Kaifeng, 475004, P. R. China

[b]Shenzhen Key Laboratory of Advanced Thin Films and Applications, Key Laboratory of Optoelectronic Devices and Systems, College of Physics and Optoelectronic Engineering, Shenzhen University, Shenzhen, 518060, P. R. China

[c]Univ Rennes, CNRS, ISCR (Institut des Sciences Chimiques de Rennes) UMR 6226, Rennes, F-35000, France

*Corresponding author

E-mail address: yuanshengjie@vip.henu.edu.cn (S.-J. Yuan); wusixin@henu.edu.cn (S.-X. Wu)

Yun-Hai Zhao and Qian-Qian Gao contributed equally to this work.

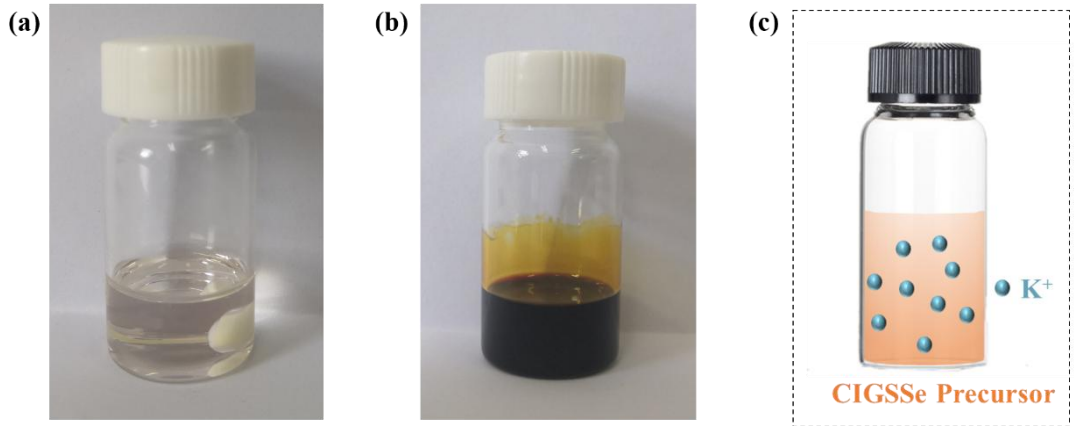

Fig. S1 Digital photograph of precursor solution: (a) the KF was dissolved in ethylenediamine and 1,2-ethanedithiol to obtain a clear and transparent solution, proving that KF can be completely dissolved in ethylenediamine and 1,2-ethanedithiol, (b) the precursor solution of CIGSSe with KF. (c) Schematic diagram of the CIGSSe precursor solution with KF, the K^+ is uniformly distributed in the solution.

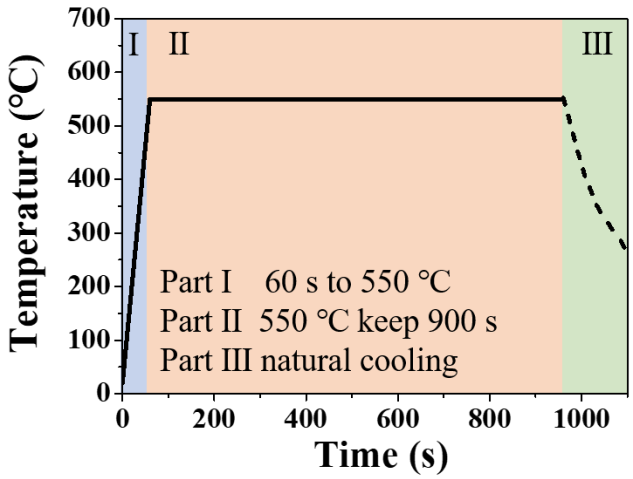

Fig. S2 Annealing profile of the CIGSSe samples.

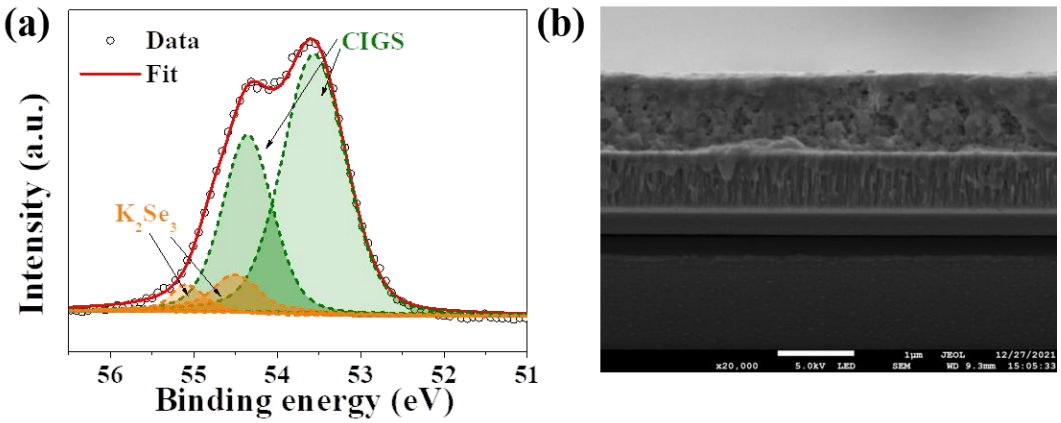

Fig. S3 The K5 sample selenized at 550 ℃ for 1 minute (a) The Se XPS spectra, (b) cross-sectional SEM image.

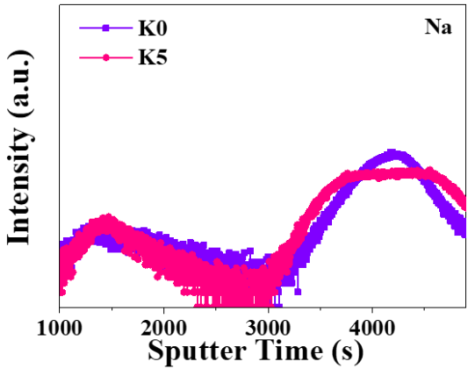

Fig. S4 TOF-SIMS of Na elemental depth profiles in K0 and K5 device.

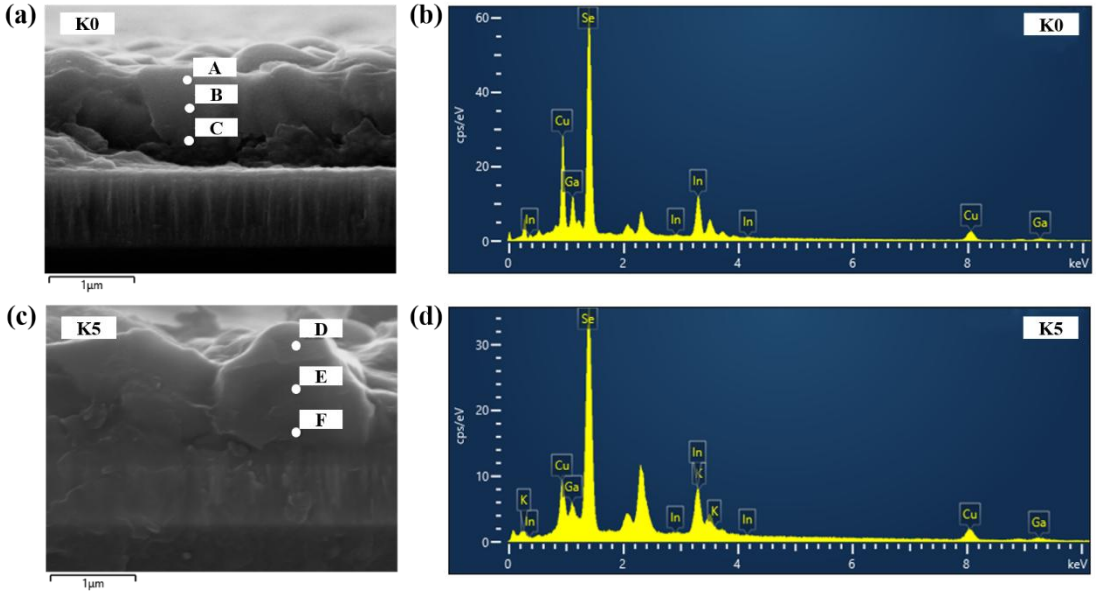

Fig. S5 Cross-sectional e SEM images of K0 sample (a) and K5 sample (b), (c) Typical EDS spectrum of the K0 sample (d) and K5 sample.

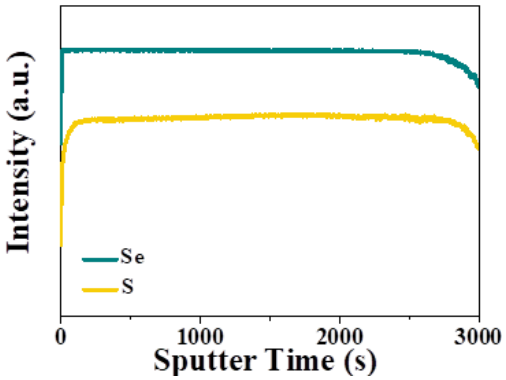

Figure S6. TOF-SIMS elemental depth profiles of Cu element in the K5 film.

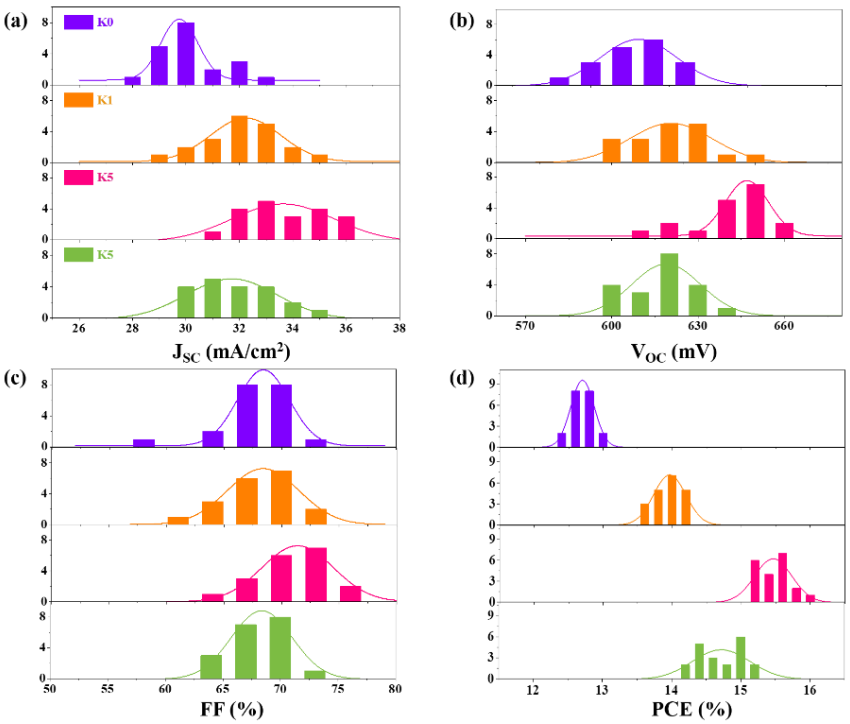

Fig. S7 Statistical distributions of photovoltaic parameters of K0-K10 devices: (a)J_{SC}, (b)V_{OC}, (c)FF, (d)PCE. Twenty cells were performed for each sample for analysis.

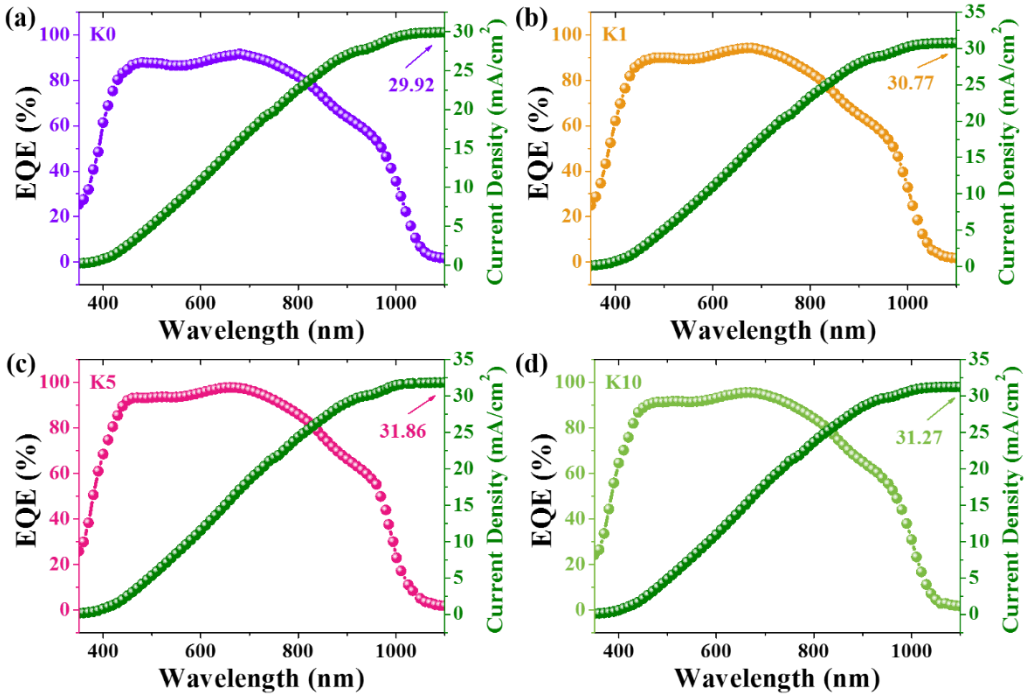

Fig. S8 Integral current calculated according to the EQE curve of K0-K10 devices.

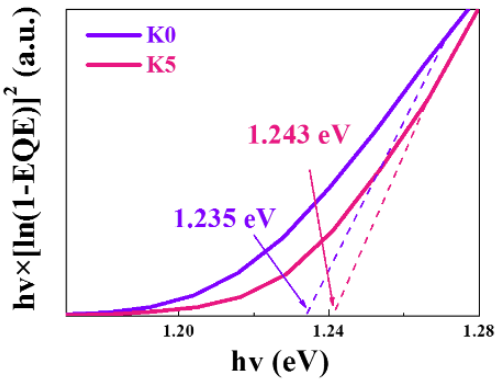

Fig. S9 The bandgap can be determined from the long wavelength absorption edge of the EQE curves by the linear extrapolation of $(E\times\ln(1-EQE))^2$ versus E_g of K0 and K5 device.

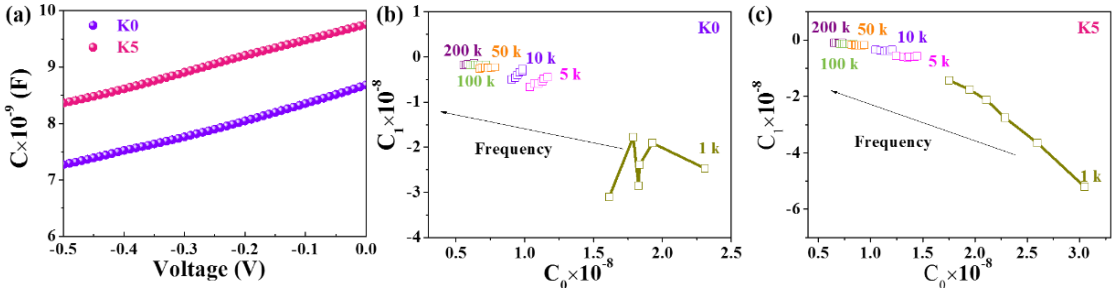

Fig. S10 (a) The C-V curves of K0 and K5 devices; (b) the measured DLCP of K0 device at different frequencies; (c) the measured DLCP of K5 device at different frequencies.

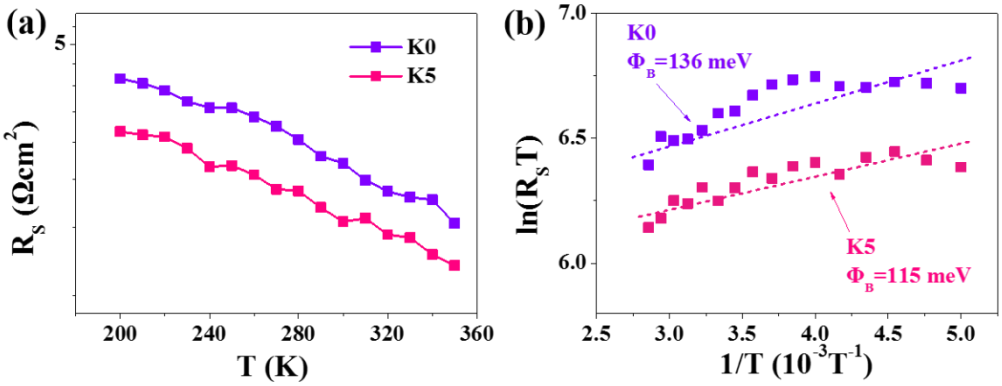

Figure S11. (a) The temperature-dependent series resistance of the K0 and K5 devices, (b) The blocking contact barrier height determination of the K0 and K5 devices.

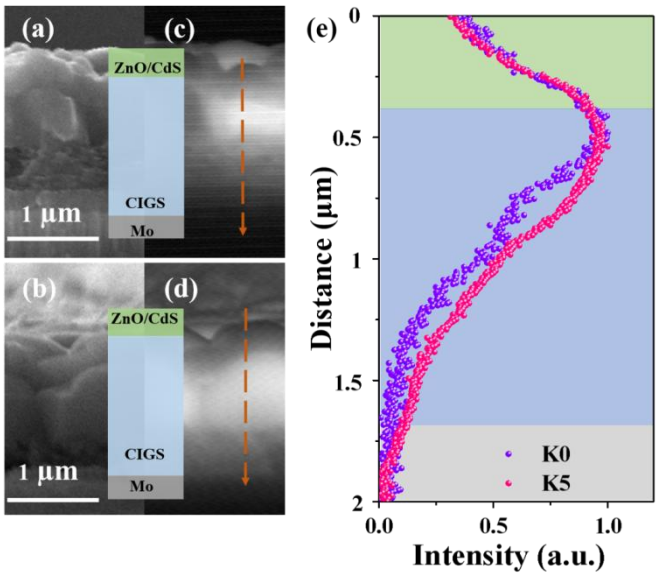

Figure S12. Cross-sectional SEM images of CIGS devices a) K0 and b) K5. The EBIC images of K0 CIGS devices (c) and K0 CIGS devices (d). (e) Normalized intensity profiling along the dashed line in (c) and (d)

Table S1 Atomic ratios of K0 sample (d) and K5 sample. measured by EDS.

Point	Cu	In	Ga	Se	K	CGI	GGI
A	22.92	16.16	8.91	52.01	-	0.91	0.36
B	22.45	15.68	8.7	53.17	-	0.92	0.36
C	21.33	15.3	8.46	54.91	-	0.90	0.36
D	22.95	16.28	9.05	51.72	0.00	0.91	0.36
E	22.62	15.75	8.86	52.77	0.00	0.92	0.36
F	22.24	16.04	8.64	53.08	0.00	0.90	0.35